Reviews in Cardiovascular Medicine

Rev. Cardiovasc. Med. **2026**; 27(11): 52089
https://doi.org/10.31083/RCM52089

Original Research

A Peri-Procedural Interpretable Machine Learning Framework to Predict Contrast-Associated Acute Kidney Injury in Older Patients: Development, Temporal Internal Validation, and Exploratory Transportability Analysis

Xishen Zhang[1], Xuan Zhang[1], Jingkun Jin[1], Jiahui Ding[1], Shanshan Li[2], Yang Xu[3,*], Wenhua Li[1,2,*]

[1]Institute of Cardiovascular Diseases, Xuzhou Medical University, 221004 Xuzhou, Jiangsu, China
[2]Department of Cardiology, Affiliated Hospital of Xuzhou Medical University, 221006 Xuzhou, Jiangsu, China
[3]Department of Cardiology, Xuzhou Central Hospital, 221009 Xuzhou, Jiangsu, China
*Correspondence: xyyx8278@163.com (Yang Xu); xzwenhua0202@163.com (Wenhua Li)
Academic Editor: Mohammad Reza Movahed
Submitted: 20 March 2026 Revised: 14 July 2026 Accepted: 20 July 2026 Published: 18 November 2026

Abstract

Background: Despite the use of low- and iso-osmolar contrast agents and rigorous hydration protocols, contrast-associated acute kidney injury (CA-AKI) remains a clinically significant complication in older patients with acute coronary syndrome (ACS). The residual risk is largely attributable to iodinated contrast media required for coronary visualization during emergent percutaneous coronary intervention (PCI). This study aimed to develop and validate an interpretable machine-learning model based on routinely available clinical features to predict CA-AKI risk in older patients with ACS. **Methods:** In this retrospective study, 2013 older ACS patients undergoing PCI were temporally divided into a training cohort (2020–2024, n = 1625) and a temporal internal validation cohort (2025, n = 388). After feature selection using the least absolute shrinkage and selection operator (LASSO) and Boruta algorithms, six machine learning algorithms were trained to predict CA-AKI. Subsequently, this study implemented a dual-tier validation strategy: a 7-variable comprehensive model for the temporal internal validation cohort and a reduced 3-variable core model for exploratory transportability analysis in an independent cohort of 755 patients from the Medical Information Mart for Intensive Care IV (MIMIC-IV) database. Model performance was evaluated using receiver operating characteristic (ROC) curves, calibration analysis, and decision curve analysis; SHapley Additive exPlanations (SHAP) were applied to enhance interpretability. **Results:** Among the six algorithms compared, the gradient boosting machine (GBM) model achieved the highest AUC and the lowest Brier score in the temporal internal validation cohort. The 7-variable model (age, lipoprotein(a) (Lp(a)), high-sensitivity C-reactive protein (hs-CRP), contrast volume, fasting glucose, pre-procedural estimated glomerular filtration rate (pre-eGFR), and pre-procedural N-terminal pro-B-type natriuretic peptide (pre-NT-proBNP)) achieved areas under the curves (AUCs) of 0.880 (95% confidence interval (CI): 0.850–0.911) in the training cohort and 0.841 (95% CI: 0.789–0.894) in the temporal internal validation cohort. In the exploratory generalizability analysis, the reduced 3-variable model applied to the MIMIC-IV database produced an AUC of 0.706 (95% CI: 0.667–0.745). An interactive web-based calculator was developed for bedside risk prediction. **Conclusion:** Incorporating Lp(a) into a temporally validated GBM framework yielded consistently strong discrimination for predicting CA-AKI in older patients with ACS. The web-based tool enables clinicians to apply risk-stratified preventive protocols at the bedside.

Keywords: lipoprotein(a); high-sensitivity C-reactive protein; older patients; acute coronary syndrome; contrast-associated acute kidney injury

1. Introduction

Percutaneous coronary intervention (PCI) is the standard treatment for acute coronary syndrome (ACS) but carries the risk of contrast-associated acute kidney injury (CA-AKI) [1]. Despite preventive measures, CA-AKI remains a common complication, particularly in older adults. Age-related renal decline and comorbidities place older patients at higher risk of nephrotoxicity, and CA-AKI is associated with worse clinical outcomes, including prolonged hospitalization and increased mortality [2].

Accurate risk stratification is essential for prevention. Traditional risk models such as the Mehran score were derived from general populations and may not fully capture the risk profile of contemporary older patients [3]. Additional biomarkers have been underutilized in this context. Lipoprotein(a) [Lp(a)], a marker with pro-inflammatory and pro-thrombotic properties, contributes to vascular injury. Chronic Lp(a)-driven endothelial impairment and a pro-thrombotic milieu render the renal microcirculation highly vulnerable. When this compromised microvasculature is then exposed to the acute osmotic and viscous insults of iodinated contrast media, a 'multiple-hit' pathogenic cascade ensues, increasing the risk of acute tubular necrosis. Beyond this, Lp(a)-related cardiovascular risk is further

Copyright: © 2026 The Author(s). Published by IMR Press.
This is an open access article under the CC BY 4.0 license.

Publisher's Note: IMR Press stays neutral with regard to jurisdictional claims in published maps and institutional affiliations.

modified by C-reactive protein [4], yet the predictive value of Lp(a) for CA-AKI in older ACS patients has not been adequately established.

Conventional logistic regression often fails to capture complex, non-linear interactions among clinical variables. Machine learning (ML) algorithms, particularly Gradient Boosting Machine (GBM), are well-suited to modeling such interactions and often yield higher predictive accuracy [5]. Many existing ML models rely on random data splitting for validation, which can overestimate performance. Temporal internal validation, which tests the model on a chronologically distinct cohort, provides a more stringent assessment of reliability against population drift in clinical practice [6].

This study aimed to develop and temporally validate a GBM model to predict CA-AKI in older ACS patients. We integrated Lp(a) with routine clinical features to improve predictive precision. To address the limited interpretability of ML algorithms, we applied the SHapley Additive exPlanations (SHAP) method. The validated algorithm was deployed as an interactive web calculator to support individualized, bedside preventive decision-making [7].

2. Materials and Methods

2.1 Study Design and Reporting Guidelines

This study—covering model development, temporal internal validation, and exploratory transportability analysis—was reported per the Transparent Reporting of a multivariable prediction model for Individual Prognosis or Diagnosis incorporating Artificial Intelligence (TRIPOD+AI) statement. A completed TRIPOD+AI checklist is provided in the **Supplementary Table 1**.

2.2 Study Population

We screened 2103 older patients (≥60 years) with acute coronary syndrome (ACS) who underwent percutaneous coronary intervention (PCI) at the Affiliated Hospital of Xuzhou Medical University between 2020 and 2025. The age threshold of 60 years corresponds to the age at which renal vulnerability becomes clinically apparent in Chinese ACS cohorts and is the criterion used in our previous nomogram for contrast-induced acute kidney injury in elderly patients with ST-segment elevation myocardial infarction [5].

Two validation cohorts were used. First, the primary cohort was temporally partitioned: patients admitted from 2020 to 2024 (n = 1625; CA-AKI events: n = 323, 19.9%) formed the training set, and those from 2025 (n = 388; CA-AKI events: n = 78, 20.1%) formed the temporal internal validation set. Second, to assess cross-geographic applicability, an exploratory transportability cohort of 755 intensive care unit (ICU) patients undergoing PCI (CA-AKI events: n = 113, 15.0%) was extracted from the Medical Information Mart for Intensive Care IV (MIMIC-IV) database. This cohort differs intentionally in disease severity and treatment pathways, allowing evaluation of the model's performance in settings with higher-acuity patients or fewer available resources.

2.3 Inclusion Criteria

Participants were eligible if they: (1) were aged ≥60 years; (2) had ACS (ST-segment elevation myocardial infarction [STEMI], non-ST-segment elevation myocardial infarction [NSTEMI], or unstable angina) diagnosed by clinical presentation, electrocardiogram (ECG), and cardiac biomarkers; (3) underwent PCI during the index hospitalization; and (4) had baseline and post-procedural renal function data required to evaluate the primary CA-AKI endpoint. Missing values for other covariates were handled via multiple imputation.

2.4 Exclusion Criteria

Patients were excluded for: (1) unavailable renal function assessment before or after PCI (including serum creatinine); (2) severe valvular disease requiring surgery; (3) ongoing systemic infection; (4) a history of malignancy; and (5) severe hepatic dysfunction. The patient selection process is summarized in Fig. 1.

2.5 Definitions

Contrast-associated acute kidney injury (CA-AKI) was defined according to modified KDIGO criteria as an increase in serum creatinine of ≥0.3 mg/dL or ≥50% above the baseline value within 3 days after PCI. The serum-creatinine thresholds are those of the KDIGO criteria; because post-procedural creatinine was reassessed over this 3-day window rather than over the 48-hour and 7-day windows of the original definition, the definition is described as modified KDIGO criteria [8]. Anemia was defined as hemoglobin <120 g/L in men or <110 g/L in non-pregnant women [9].

Risk stratification for contrast-related nephropathy was performed using the 2004 Mehran risk score, which assigns weighted points to hemodynamic instability (hypotension and intra-aortic balloon pump use), heart failure, age >75 years, diabetes, anemia, contrast volume, and baseline renal function. Patients are classified into low, moderate, high, and very high risk categories. The Mehran 2 (2021) pre-procedural score was also calculated from baseline variables: ACS, cardiac function (heart failure or reduced ejection fraction), chronic kidney disease stage, diabetes, anemia, and age ≥75 years. Patients were categorized into four corresponding risk strata [10].

2.6 Data Preprocessing

All data were retrieved from the institution's electronic medical record system. Baseline characteristics included age, sex, smoking status, and comorbidities. Pre-procedural laboratory tests were obtained within 24 hours before PCI, preferentially closest to the index procedure.

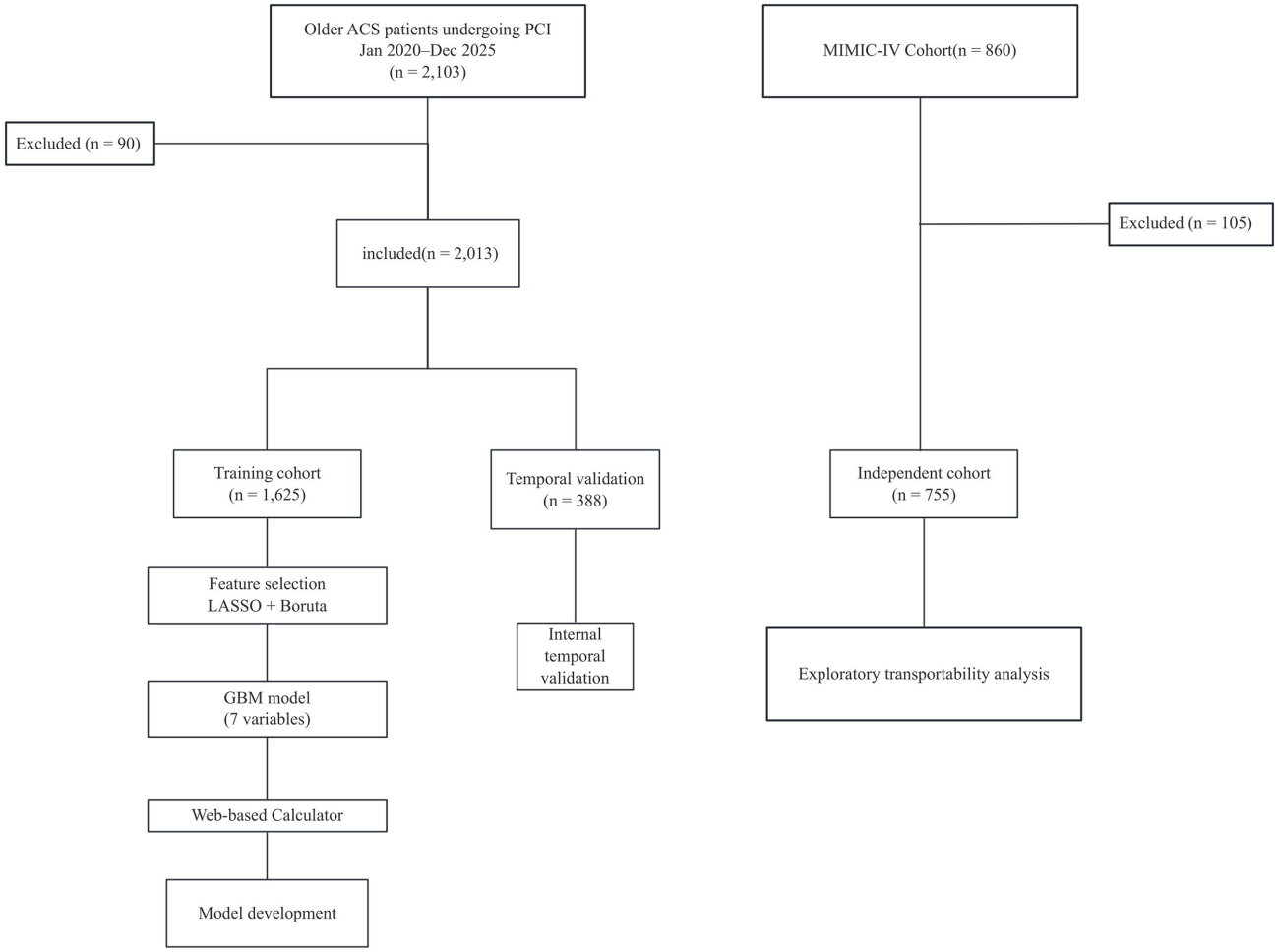


Fig. 1. Flowchart detailing the patient selection and statistical analysis workflow for older ACS patients undergoing PCI. Abbreviations: ACS, acute coronary syndrome; GBM, gradient boosting machine; LASSO, least absolute shrinkage and selection operator; MIMIC-IV, Medical Information Mart for Intensive Care IV; PCI, percutaneous coronary intervention.

These included routine hematology and biochemistry parameters: white blood cell count, red blood cell count, hemoglobin, platelet count, total bilirubin, albumin, fasting glucose, serum creatinine, high-sensitivity C-reactive protein (hs-CRP), Lp(a), and other routinely measured indices. Variables with >30% missingness were excluded.

To prevent data leakage, the dataset was temporally split into a training cohort (n = 1625; 2020–2024) and an internal validation cohort (n = 388; 2025) before imputation. Missing values were then handled by multiple imputation using chained equations (MICE), applied independently within each cohort. The missing proportions for the seven final core predictors were consistently low: Age (0%), Contrast Volume (0%), Fasting Glucose (4.0%), eGFR (3.1%), N-terminal pro-B-type natriuretic peptide (NT-proBNP) (1.8%), hs-CRP (2.4%), and Lp(a) (2.8%). The Missing at Random (MAR) assumption cannot be formally tested. We supported it through clinical context and missingness pattern exploration. Core biomarkers (pre-procedural NT-proBNP, hs-CRP, and Lp(a)) are mandated routine assessments for older ACS patients at our institution. Their minimal missingness was therefore attributed to administrative logistics rather than disease severity. Baseline characteristics were comparable between complete-case and missing-data patients, further supporting the MAR assumption.

2.7 Statistical Analysis

All statistical analyses and model development were conducted in R (version 4.5.2; R Foundation for Statistical Computing, Vienna, Austria). Missing data were imputed using the MICE package, generating 5 imputed datasets (m = 5) over 50 iterations (maxit = 50). Predictive mean matching (PMM) was applied for continuous variables to preserve physiological non-linear distributions. A pre-specified sensitivity analysis used a complete-case analysis (CCA) approach, retraining and evaluating models exclusively on patients with no missing core predictors.

Continuous variables are reported as mean ± standard deviation (normally distributed) or median (interquartile range) (non-normally distributed). Group comparisons used the independent-samples *t*-test or Mann–Whitney U

test as appropriate. Categorical variables are presented as counts (percentages) and compared by the chi-square test.

Predictor selection combined Boruta for initial screening with least absolute shrinkage and selection operator (LASSO) regression for regularization. Collinearity was assessed via variance inflation factor (VIF). Six machine learning algorithms were developed from the selected features: logistic regression (LR), neural networks (NN), random forest (RF), support vector machine (SVM), GBM, and extreme gradient boosting (XGBoost). A global random seed (set.seed(2026)) was set across all data splitting, cross-validation, and model training. The R packages used were stats (LR), RF, e1071 (SVM), gbm (GBM), xgboost (XGBoost), and nnet (NN).

Hyperparameters for all ML algorithms were tuned by grid search with 10-fold cross-validation within the development cohort. The final hyperparameters for each algorithm are listed in **Supplementary Table 2**. Given the moderate class imbalance in the training cohort (CA-AKI to non-CA-AKI ratio ≈ 1:4), we optimized using the Area Under the Curve (AUC), which is insensitive to class imbalance, rather than accuracy. No artificial resampling (e.g., Synthetic Minority Over-sampling Technique [SMOTE]) was applied, preserving the clinical predictor distributions as observed.

Models were evaluated on discrimination (AUC, accuracy), calibration (Brier score, calibration curves), and clinical net benefit (decision curve analysis [DCA]). Binary classification metrics—sensitivity, specificity, and accuracy—were derived after threshold optimization by Youden's Index. The GBM model was compared against the Mehran 2004 and Mehran 2021 risk scores using receiver operating characteristic (ROC) curves (AUCs compared by DeLong's test), calibration plots, and DCA.

Continuous net reclassification improvement (NRI) and integrated discrimination improvement (IDI) served two purposes. First, they assessed the incremental value of adding Lp(a) and hs-CRP to a clinical baseline model (age, pre-procedural eGFR, contrast volume, fasting glucose, pre-procedural NT-proBNP). Second, they quantified the reclassification and discrimination gains of the GBM model over the traditional Mehran scores.

Model interpretability was assessed using SHAP, which provides both global feature importance and case-level explanations. All validation cohorts met the established threshold of at least 10 events per predictor variable (EPV): temporal validation EPV = 11.1; MIMIC-IV validation EPV = 37.6. A two-sided $p < 0.05$ was considered statistically significant.

3. Results

3.1 Baseline Characteristics

Patients in the training set were stratified into non-CA-AKI (n = 1302) and CA-AKI (n = 323) groups per the diagnostic criteria. The two groups differed across multiple baseline demographics, comorbidities, and laboratory parameters, including the core predictors eGFR, fasting glucose, NT-proBNP, hs-CRP, and Lp(a). Detailed baseline characteristics are presented in Table 1. A comparison of baseline characteristics across the training, temporal internal validation, and MIMIC-IV exploratory transportability cohorts is presented in **Supplementary Table 3**.

3.2 Feature Selection

We screened 69 candidate predictors using a resampling-based hybrid feature-selection protocol. All model development—feature screening, hyperparameter tuning, and internal resampling—was confined to the training cohort (2020–2024). The temporal validation cohort (2025) was held out entirely from model building and threshold selection.

Within the training cohort, we applied a dual-algorithm consensus strategy with bootstrap resampling. The Boruta algorithm ran for 500 maximal iterations (maxRuns = 500) with 100 bootstrap resampling iterations to capture linear and non-linear associations (Fig. 2). The 100-iteration limit balanced algorithmic convergence with computational feasibility. LASSO regression with 500 bootstrap resampling iterations was then applied for regularization and to address multicollinearity (Fig. 3). Features were ranked by selection frequency: 100 bootstraps for Boruta (Fig. 4A) and 500 bootstraps for LASSO (Fig. 4B).

The intersection of the two top-20 sets yielded seven core variables: age, lipoprotein(a) [Lp(a)], contrast volume, pre-procedural eGFR, hs-CRP, pre-procedural NT-proBNP, and fasting glucose. All variance inflation factors (VIFs) were below 5, and pairwise Spearman rank correlations confirmed independence among the selected predictors (Fig. 5). With this 7-predictor set finalized, six machine learning algorithms (GBM, logistic regression, neural network, random forest, SVM, and XGBoost) were developed and compared within the training cohort. The GBM architecture was then evaluated in the independent validation cohorts.

3.3 Model Performance Comparison

GBM was selected as the final model. Random forest achieved a slightly higher training AUC (0.899) but showed signs of overfitting, with its validation AUC falling to 0.825. GBM maintained more consistent discrimination across cohorts: an AUC of 0.880 (95% CI: 0.850–0.911) in training and 0.841 (95% CI: 0.789–0.894) in temporal validation (Fig. 6A). The complete-case sensitivity analysis produced similar results (training AUC = 0.872; validation AUC = 0.839), indicating that MICE imputation did not bias predictive accuracy.

GBM also showed the best calibration in the validation set, with the lowest Brier score (0.083) and calibration parameters close to ideal (intercept = −0.109; slope = 1.036)

Table 1. Baseline characteristics of patients in the training cohort stratified by contrast-associated acute kidney injury (CA-AKI) status.

Characteristic	No CA-AKI (n = 1302)	CA-AKI (n = 323)	*p* value
Demographics			
Age (years)	67 [64, 75]	69 [67, 77]	0.005
Female sex (n%)	277 (21.3)	111 (34.4)	<0.001
Height (cm)	168 [162, 172]	167 [160, 170]	0.028
Weight (kg)	70 [60, 80]	70 [60, 80]	0.360
Comorbidities			
Hypertension (n%)	589 (45.2)	150 (46.4)	0.698
Diabetes mellitus (n%)	334 (25.7)	95 (29.4)	0.170
Chronic kidney disease (n%)	36 (2.8)	14 (4.3)	0.144
Hypotension (n%)	40 (3.1)	15 (4.6)	0.162
Anemia (n%)	65 (5.0)	27 (8.4)	0.019
Previous myocardial infarction (n%)	86 (6.6)	36 (11.1)	0.006
Smoking (n%)	259 (19.9)	126 (39.0)	<0.001
Clinical presentation			
Heart rate (bpm)	80 [72, 90]	82 [72, 91]	0.218
Killip class (n%)			0.002
I	1113 (85.5)	255 (78.9)	
II	83 (6.4)	24 (7.4)	
III	17 (1.3)	2 (0.6)	
IV	89 (6.8)	42 (13.0)	
LVEF (%)	51 [48, 56]	51 [46, 53]	<0.001
IABP use (n%)	111 (8.5)	33 (10.2)	0.338
Procedure-related			
Procedure duration (min)	60 [45, 70]	60 [50, 70]	0.309
Contrast agent type (n%)			<0.001
Ioversol	277 (21.3)	111 (34.4)	
Iodixanol	1025 (78.7)	212 (65.6)	
Contrast agent volume (n%)			0.006
<100 mL	1117 (85.8)	257 (79.6)	
≥100 mL	185 (14.2)	66 (20.4)	
Medications			
Aspirin (n%)	1292 (99.2)	315 (97.5)	0.015†
P2Y12 inhibitor (n%)	1282 (98.5)	316 (97.8)	0.427
Statin (n%)	1290 (99.1)	320 (99.1)	1.000†
ACEI/ARB (n%)	683 (52.5)	167 (51.7)	0.808
Beta-blocker (n%)	1112 (85.4)	267 (82.7)	0.218
Nitrates (n%)	578 (44.4)	154 (47.7)	0.288
Low-molecular-weight heparin (n%)	978 (75.1)	247 (76.5)	0.613
Calcium channel blocker (n%)	397 (30.5)	111 (34.4)	0.179
Diuretics (n%)	640 (49.2)	232 (71.8)	<0.001
Laboratory parameters			
White blood cell count ($\times 10^9$/L)	9.90 [8.00, 12.00]	10.10 [8.40, 12.20]	0.310
Neutrophil count ($\times 10^9$/L)	7.55 [5.61, 9.82]	8.30 [6.52, 10.35]	0.001
Lymphocyte count ($\times 10^9$/L)	1.40 [1.00, 2.10]	1.20 [0.80, 1.60]	<0.001
Monocyte count ($\times 10^9$/L)	0.50 [0.36, 0.68]	0.43 [0.29, 0.60]	<0.001
Red blood cell count ($\times 10^{12}$/L)	4.60 [4.21, 5.00]	4.55 [4.05, 4.92]	0.044
Hemoglobin (g/L)	141 [129, 153]	138 [123, 149]	0.009
Hematocrit (%)	42.80 [39.38, 45.90]	41.90 [37.65, 44.95]	0.012
Platelet count ($\times 10^9$/L)	209 [175, 251]	202 [174, 239]	0.098
Mean platelet volume (fL)	10 [9, 11]	10 [9, 11]	0.318
hs-CRP (mg/L)	2.30 [1.10, 5.55]	3.20 [1.40, 7.35]	0.005

Table 1. Continued.

Characteristic	No CA-AKI (n = 1302)	CA-AKI (n = 323)	*p* value
SII	1122 [599, 1859]	1383 [924, 2161]	<0.001
SIRI	2.46 [1.37, 4.48]	2.85 [1.81, 4.67]	0.023
Fibrinogen (g/L)	2.73 [2.28, 3.33]	2.68 [2.21, 3.40]	0.239
D-dimer (μg/mL)	0.34 [0.20, 0.85]	0.47 [0.26, 0.95]	0.004
AT III (%)	87.00 [79.00, 94.62]	86.00 [78.50, 93.05]	0.238
FDP (μg/mL)	2.20 [1.60, 3.60]	2.60 [1.80, 4.10]	<0.001
Serum creatinine (μmol/L)	57 [47, 68]	65 [54, 76]	<0.001
Serum uric acid (μmol/L)	313 [257, 380]	291 [229, 340]	<0.001
blood urea nitrogen (mmol/L)	5.69 [4.75, 6.98]	5.83 [4.72, 7.16]	0.504
eGFR [mL/(min·1.73 m^2)]	124 [96, 153]	110 [89, 130]	<0.001
Cys C (mg/L)	0.87 [0.62, 1.19]	0.89 [0.68, 1.31]	0.543
Albumin (g/L)	38.10 [35.40, 40.62]	38.20 [35.85, 41.15]	0.507
Prealbumin (g/L)	0.21 [0.18, 0.25]	0.21 [0.17, 0.25]	0.789
LDH (U/L)	491 [298, 722]	571 [372, 946]	0.001
CK (U/L)	286 [102, 973]	621 [174, 1355]	<0.001
CK-MB (U/L)	18 [4, 90]	45 [10, 125]	<0.001
hs-TnT (pg/mL)	276 [38, 1549]	637 [103, 2009]	<0.001
Pre-procedure NT-proBNP (pg/mL)	405 [110, 1554]	549 [208, 1677]	0.004
Fasting blood glucose (mmol/L)	5.93 [5.17, 7.66]	6.44 [5.38, 8.57]	0.001
HbA1C (%)	6.00 [5.20, 7.90]	6.50 [5.90, 8.70]	0.401
Total bilirubin (μmol/L)	13 [10, 18]	15 [10, 21]	0.041
Direct bilirubin (μmol/L)	5.2 [4.0, 6.8]	5.6 [4.3, 7.8]	0.007
Total cholesterol (mmol/L)	4.22 [3.63, 4.89]	4.35 [3.73, 5.21]	0.039
Triglycerides (mmol/L)	1.25 [0.88, 1.81]	1.30 [0.91, 1.86]	0.218
HDL-cholesterol (mmol/L)	0.94 [0.81, 1.12]	1.03 [0.84, 1.23]	0.003
LDL-cholesterol (mmol/L)	2.63 [2.11, 3.22]	2.83 [2.18, 3.52]	0.015
Sd-LDL (mmol/L)	0.74 [0.51, 1.09]	0.80 [0.52, 1.21]	0.329
Lipoprotein(a) (mg/L)	220.00 [143.00, 365.75]	295.00 [241.00, 425.37]	0.002
Apolipoprotein A (g/L)	1.07 [0.95, 1.22]	1.11 [0.98, 1.28]	0.010
Apolipoprotein B (g/L)	0.89 [0.74, 1.06]	0.94 [0.75, 1.13]	0.054
Risk scores			
Mehran 2004 score	3.00 [0.00, 5.00]	3.00 [1.00, 6.00]	0.001
Mehran 2021 score	4.00 [4.00, 6.00]	5.00 [4.00, 6.00]	<0.001

Categorical variables were compared using Pearson's chi-square test; †Fisher's exact test where any expected count was below 5. Abbreviations: LVEF, left ventricular ejection fraction; hs-CRP, high-sensitivity C-reactive protein; FDP, fibrinogen degradation products; eGFR, estimated glomerular filtration rate; CK, creatine kinase; CK-MB, creatine kinase-MB; NT-proBNP, N-terminal pro-B-type natriuretic peptide; hs-TnT, high-sensitivity troponin T; TG, triglycerides; LDH, lactate dehydrogenase; IABP, intra-aortic balloon pump; SIRI, systemic inflammation response index; SII, systemic immune-inflammation index; sd-LDL, small dense low density lipoprotein cholesterol; HbA1C, hemoglobin A1c; Cys C, cystatin C; AT III, antithrombin III; HDL, high-density lipoprotein; ACEI/ARB, angiotensin-converting enzyme inhibitor/angiotensin receptor blocker.

(Fig. 6B, Table 2). On decision curve analysis, the GBM model yielded positive net benefit across a threshold probability range of 5% to 74% in the validation set (Fig. 6C). The range from 5% to 30% is clinically relevant: this is where thresholds for initiating preventive measures, such as intensive fluid hydration or contrast volume restriction, typically lie. A positive net benefit in this zone indicates the model identifies high-risk patients while sparing low-risk patients from unnecessary interventions. Across algorithms, 10-fold cross-validation showed minor AUC fluctuations, but temporal hold-out validation supported GBM as the most reliable choice (Fig. 7).

3.3.1 Incremental Predictive Value of the Full Model

The baseline model provided reasonable discrimination. Adding Lp(a) and hs-CRP improved risk stratification. In the validation cohort, the full 7-variable model yielded a continuous NRI of 0.2322 (95% CI: 0.0022–0.4623, $p = 0.0479$) and an IDI of 0.012 (95% CI: 0.002–0.022, $p = 0.0164$) over the baseline. Improvements in the

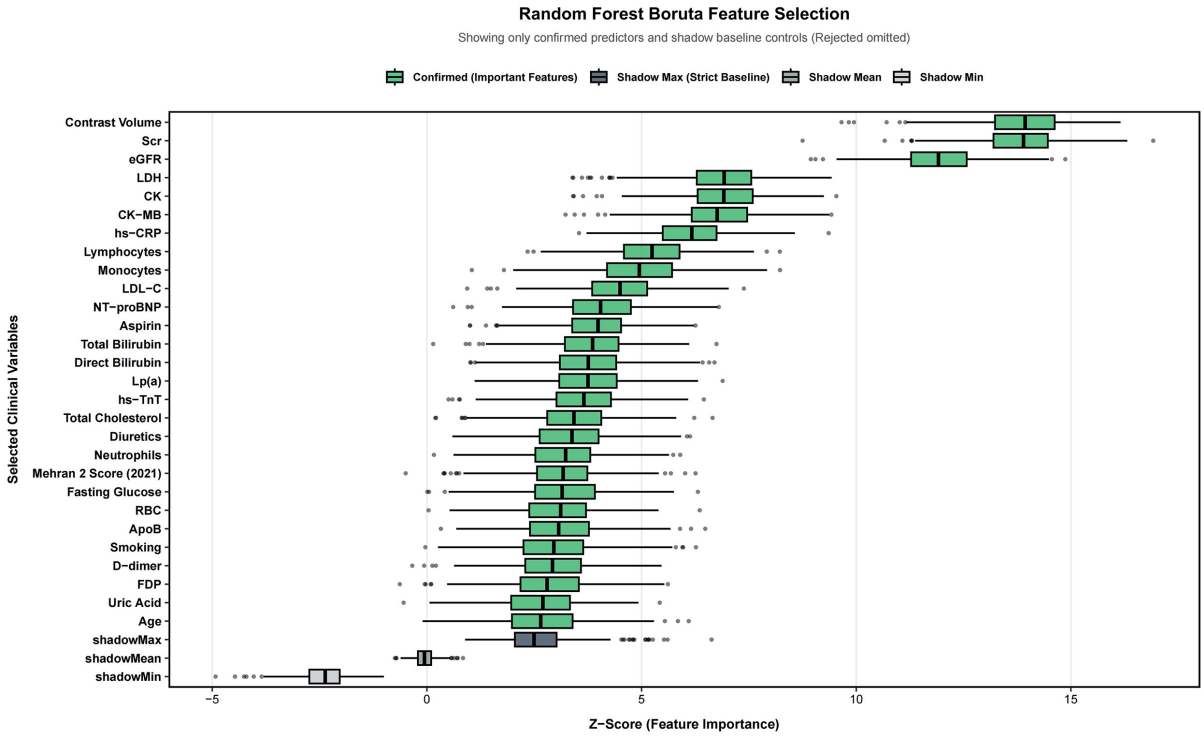


Fig. 2. Feature importance ranking identified by the Boruta algorithm. Abbreviations: ApoB, apolipoprotein B; CK, creatine kinase; eGFR, estimated glomerular filtration rate; FDP, fibrinogen degradation products; hs-CRP, high-sensitivity C-reactive protein; hs-TnT, high-sensitivity troponin T; LDH, lactate dehydrogenase; LDL-C, low-density lipoprotein cholesterol; Lp(a), lipoprotein(a); NT-proBNP, N-terminal pro-B-type natriuretic peptide; RBC, red blood cell.

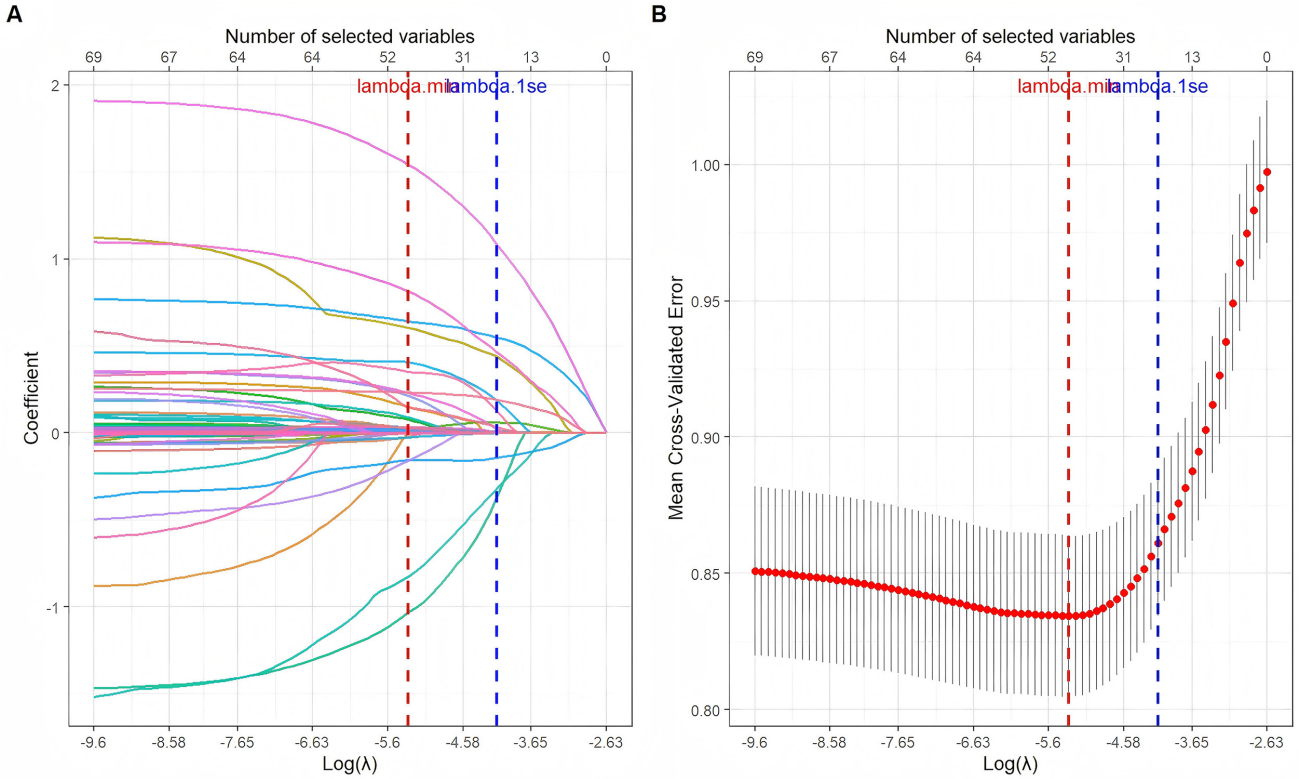


Fig. 3. Feature selection using LASSO regression. (A) Coefficient profiles of the candidate variables. (B) Selection of the optimal tuning parameter via 10-fold cross-validation. Abbreviations: LASSO, least absolute shrinkage and selection operator.

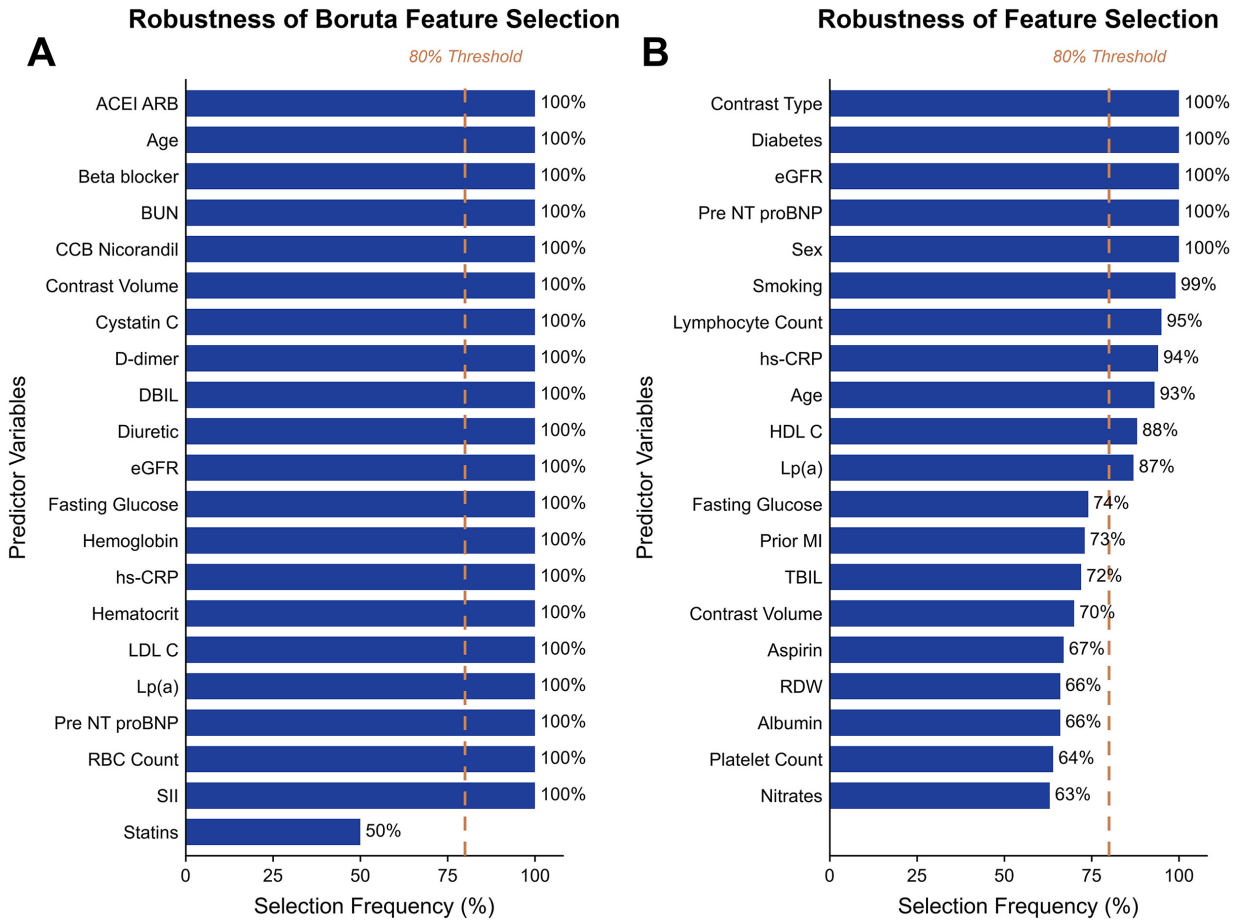


Fig. 4. Feature selection via dual-algorithm bootstrap consensus. (A) Top 20 variables ranked by selection frequency across 100 Boruta bootstrap iterations. (B) Top 20 variables across 500 LASSO bootstrap iterations. Red dashed lines indicate the 80% threshold. The final seven predictors were determined by intersecting the top variables from both algorithms. Abbreviations: ACEI/ARB, angiotensin-converting enzyme inhibitor/angiotensin receptor blocker; BUN, blood urea nitrogen; CCB, calcium channel blocker; DBIL, direct bilirubin; eGFR, estimated glomerular filtration rate; HDL-C, high-density lipoprotein cholesterol; hs-CRP, high-sensitivity C-reactive protein; LASSO, least absolute shrinkage and selection operator; LDL-C, low-density lipoprotein cholesterol; Lp(a), lipoprotein(a); NT-proBNP, N-terminal pro-B-type natriuretic peptide; RBC, red blood cell; RDW, red blood cell distribution width; SII, systemic immune-inflammation index.

training cohort were similar (continuous NRI: 0.263, p = 0.0359; IDI: 0.015, p = 0.043). The inclusion of Lp(a) and hs-CRP thus provided a statistically significant net gain in reclassifying patients' CA-AKI risk.

3.3.2 Comparison With Established Clinical Risk Scores

The 7-variable GBM model was compared against the Mehran 2004 and Mehran 2021 scores. In the training cohort, GBM (AUC = 0.880) outperformed both Mehran 2004 (AUC = 0.690, DeLong $p < 0.001$) and Mehran 2021 (AUC = 0.696, DeLong $p < 0.001$) (Fig. 8A). This gap held in temporal internal validation: GBM AUC = 0.841 versus Mehran 2004 AUC = 0.653 (DeLong $p < 0.001$) and Mehran 2021 AUC = 0.695 (DeLong $p < 0.001$).

The GBM model also improved risk reclassification in the validation cohort. Against the Mehran 2004 score, it produced a continuous NRI of 1.246 ($p < 0.001$) and an IDI of 0.284 ($p < 0.001$). Against Mehran 2021, the corresponding values were continuous NRI = 0.973 ($p < 0.001$) and IDI = 0.179 ($p < 0.001$).

Loess-smoothed calibration curves showed that GBM maintained accurate probability estimates across both cohorts, while the Mehran scores exhibited calibration drift (Fig. 8B). On decision curve analysis, GBM yielded higher net benefit than both traditional scores across threshold probabilities of 5% to 40%—the range in which clinicians decide whether to initiate peri-procedural preventive protocols (Fig. 8C).

3.3.3 Exploratory Analysis in a Restricted-Feature Cohort

We used the independent MIMIC-IV database to explore the generalizability of the core predictors. Lp(a), hs-CRP, NT-proBNP, and contrast volume were largely unrecorded in MIMIC-IV, precluding a formal transportability

Table 2. Predictive performance metrics of the six machine learning models in the training and temporal internal validation cohorts.

Data set	Model	AUC	Accuracy	Sensitivity	Specificity	Brier score	Intercept	Slope
Training	GBM	0.880	0.792	0.839	0.780	0.089	0.249	1.200
	Logistic Regression	0.831	0.816	0.650	0.857	0.101	0.000	1.000
	Neural Network	0.869	0.827	0.720	0.853	0.093	0.099	1.087
	Random Forest	0.899	0.882	0.748	0.915	0.086	0.248	0.283
	SVM	0.866	0.854	0.790	0.870	0.084	0.000	1.096
	XGBoost	0.835	0.877	0.811	0.893	0.067	0.252	1.192
Validation	GBM	0.841	0.818	0.750	0.835	0.083	–0.109	1.036
	Logistic Regression	0.812	0.750	0.800	0.738	0.112	–0.262	0.824
	Neural Network	0.818	0.718	0.867	0.680	0.100	–0.285	0.782
	RF	0.825	0.862	0.650	0.915	0.100	–0.868	0.119
	SVM	0.790	0.833	0.667	0.875	0.106	–0.619	0.690
	XGBoost	0.809	0.805	0.700	0.832	0.089	0.005	0.931

Abbreviations: AUC, area under the curve; GBM, gradient boosting machine; LR, logistic regression; NN, neural network; RF, random forest; SVM, support vector machine; XGBoost, extreme gradient boosting.

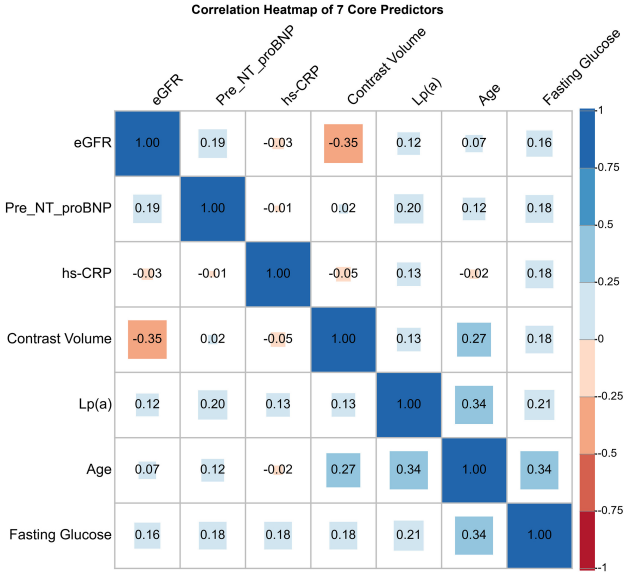


Fig. 5. Spearman correlation heatmap of the candidate variables in the training cohort. Abbreviations: eGFR, estimated glomerular filtration rate; hs-CRP, high-sensitivity C-reactive protein; Lp(a), lipoprotein(a); NT-proBNP, N-terminal pro-B-type natriuretic peptide.

analysis under TRIPOD+AI guidelines. We therefore tested a reduced-feature GBM model using the three universally available predictors: age, pre-procedural eGFR, and fasting glucose.

CA-AKI incidence in the MIMIC-IV cohort was lower than in the primary cohort (15.0% vs. 20.1%), likely reflecting stricter contrast volume restriction and intensive hemodynamic monitoring typical of ICU settings. Despite the reduced feature set and the lower event rate, the 3-variable model achieved an AUC of 0.706 (95% CI: 0.667–0.745) in the MIMIC-IV cohort; the corresponding training-cohort AUC was 0.749 (95% CI: 0.718–0.780) (Fig. 9A) with satisfactory calibration (Fig. 9B). DCA showed positive net benefit across a threshold probability range of approximately 10% to 45% (Fig. 9C).

In the ICU, where patients already carry elevated baseline risk for acute kidney injury and fluid balance is tightly managed, a net benefit in this range suggests the simplified model can still inform decisions, such as using contrast-sparing techniques or adjusting hemodynamics, when detailed biomarkers are unavailable.

4. Feature Importance on Prediction

SHAP (SHapley Additive exPlanations) analysis was applied to the optimized GBM model to quantify each predictor's contribution and directionality for CA-AKI risk. By mean absolute SHAP value, pre-procedural eGFR and age were the strongest predictors (Fig. 10A). Contrast volume, Log10_NT-proBNP, hs-CRP, Lp(a), and fasting glucose followed. The SHAP summary beeswarm plot (Fig. 10B) shows the direction of these associations at the individual level. Lower baseline eGFR (dark purple points) was linked to positive SHAP values, indicating higher predicted CA-AKI risk. Higher values (yellow points) for age, contrast volume, NT-proBNP, hs-CRP, Lp(a), and fasting glucose shifted model output in the positive direction. The SHAP dependence plots (Fig. 10C) reveal non-linear patterns. The risk contribution of eGFR accelerated as renal function declined below normal thresholds. Age showed a sharp risk increase at older extremes. Biomarkers such as NT-proBNP and Lp(a), and contrast volume, exhibited threshold effects at higher levels—the model learned decision boundaries specific to the older ACS cohort. At the individual case level, these features produced patient-specific risk profiles (Fig. 10D,E).

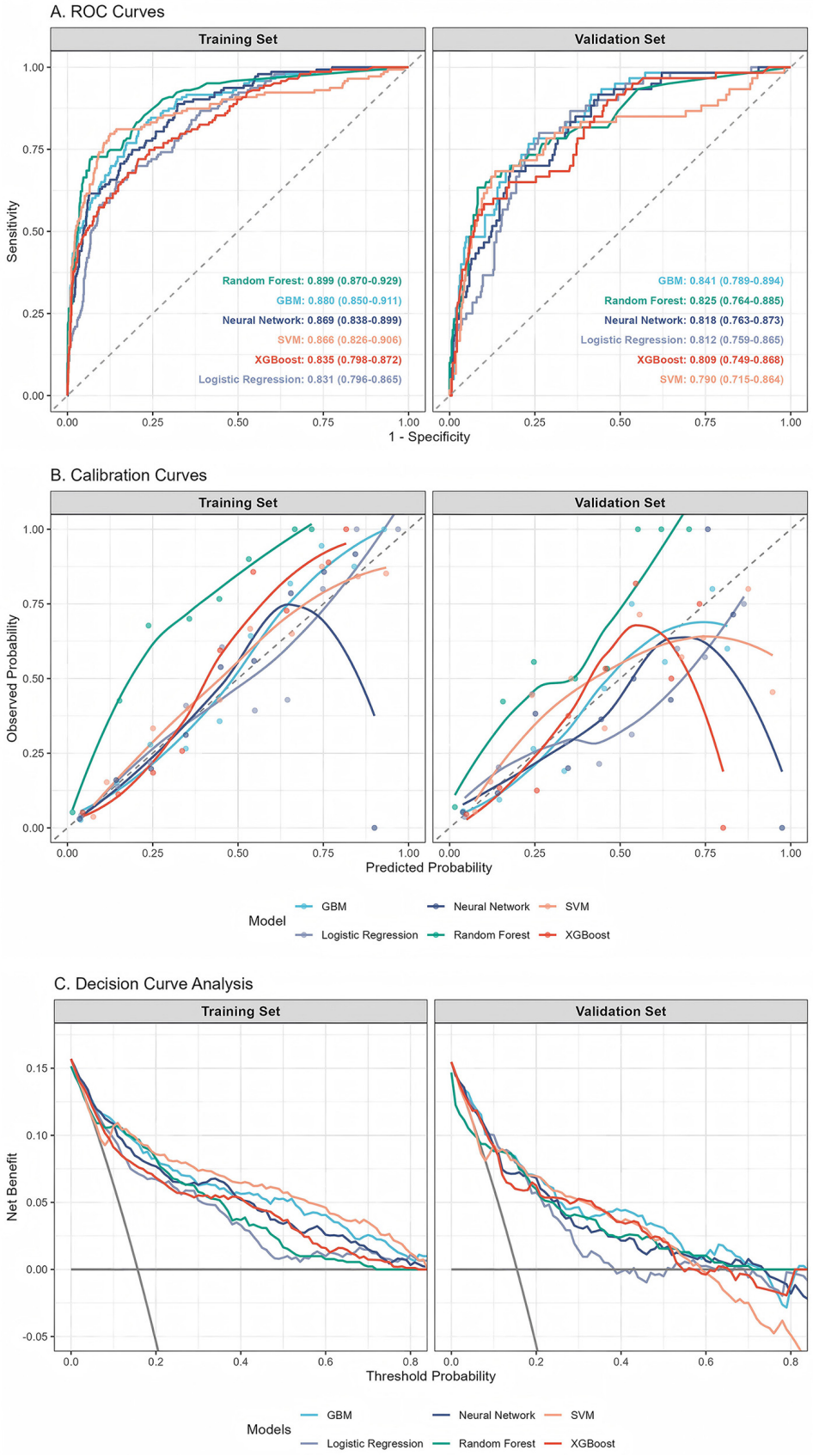


Fig. 6. Predictive performance of the established machine learning models. (A) Receiver operating characteristic (ROC) curves. (B) Calibration plots. (C) Decision curve analysis (DCA). Abbreviations: AUC, area under the curve; DCA, decision curve analysis; GBM, gradient boosting machine; ROC, receiver operating characteristic; SVM, support vector machine; XGBoost, extreme gradient boosting.

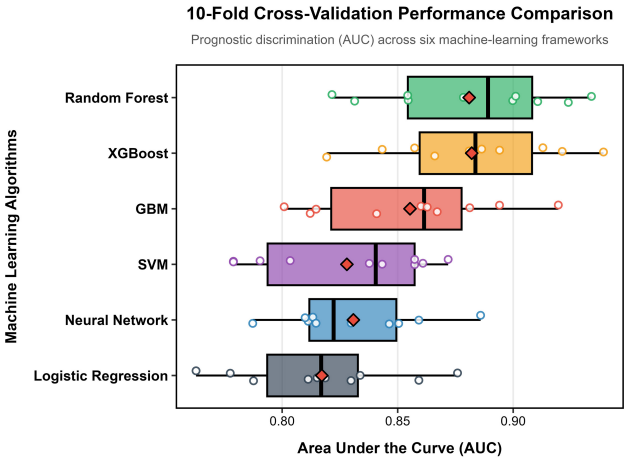


Fig. 7. Ten-fold cross-validation performance across different machine learning models. Abbreviations: AUC, area under the curve; GBM, gradient boosting machine; SVM, support vector machine; XGBoost, extreme gradient boosting.

5. Development and Deployment of a Web-Based Clinical Calculator

The optimized GBM model was deployed as an interactive web calculator (Fig. 11; https://zhangxishen.shinyapps.io/CIAKI_Predictor_Plus/). The application supports a two-stage, peri-procedural assessment using seven core predictors: age, pre-procedural eGFR, NT-proBNP, hs-CRP, Lp(a), fasting glucose, and contrast volume. Before PCI, clinicians can enter an estimated contrast volume to simulate risk. If the predicted risk is high, this prompts stricter contrast-sparing technique during the procedure. After PCI, the field is updated with the actual administered volume, yielding a definitive CA-AKI probability. The calculator allows clinicians to stratify risk at the bedside and adjust downstream interventions, such as individualized hydration protocols, for older ACS patients.

6. Discussion

We developed and validated a machine learning framework to predict individualized CA-AKI risk in older ACS patients undergoing PCI [11]. From 69 candidate parameters, a consensus feature-selection protocol identified seven core predictors: age, pre-procedural eGFR, contrast volume, NT-proBNP, hs-CRP, Lp(a), and fasting glucose [12]. Among six algorithms tested, GBM achieved the highest AUC and the lowest Brier score in the temporal internal validation cohort, and was therefore selected as the final model. In previous machine-learning studies of contrast-induced acute kidney injury, tree-based ensembles have also outperformed logistic regression, although the best-performing algorithm has varied between cohorts; in one multicentre series of patients with acute myocardial infarction, random forest ranked first [13]. The full 7-variable model performed well in temporal internal validation, and a reduced-feature model confirmed that the core predictors generalized in an exploratory analysis of the MIMIC-IV database [14]. SHAP interpretability and a web-based calculator make the model accessible at the bedside [15].

Our earlier work produced a linear nomogram for CA-AKI in an emergent STEMI cohort [5], but the current study differs in three respects. First, the target population now covers the broader ACS spectrum, which allows pre-procedural biomarker profiling and hydration; these strategies are rarely feasible in hyper-acute STEMI. Second, we moved from linear modeling to a non-linear GBM. SHAP analysis showed that GBM captures risk thresholds that nomograms miss. Third, we replaced a static scoring tool with a two-stage peri-procedural web calculator that updates risk after the actual contrast volume is entered. The MIMIC-IV analysis tests the baseline performance of this non-linear framework under constrained conditions.

Our feature-selection strategy, intersecting the top features from Boruta and LASSO with bootstrap resampling, isolated stable predictors and eliminated collinearity [16,17]. On this feature space, GBM outperformed logistic regression and other ML methods [18]. The advantage of tree-based ensemble methods reflects a clinical observation: CA-AKI in older patients is not an additive accumulation of independent risk factors. It arises from non-linear interactions among metabolic stress, hemodynamic compromise, and declining renal reserve that linear models do not capture [19].

SHAP analysis was used to examine how variables contributed to model output, not to establish causal mechanisms [20]. The resulting feature importances are consistent with known pathophysiology. Pre-procedural eGFR and age were the strongest predictors, reflecting the baseline vulnerability of aging kidneys. The SHAP dependence plots showed non-linear, threshold-like risk escalations for Lp(a), highlighting the potential role of the immuno-lipid axis in renal microvascular injury.

The biological rationale for the prominence of Lp(a) is plausible but remains inferential, and the present study was not designed to test any mechanistic pathway. In human plasma, Lp(a) is the principal carrier of pro-inflammatory oxidized phospholipids (OxPLs), which promote a pro-inflammatory vascular phenotype through monocyte recruitment and upregulation of adhesion molecules [21]. Elevated Lp(a) has also been associated with impaired endothelium-dependent vasomotor function in humans, consistent with reduced nitric oxide bioavailability [22]. Clinically, higher pre-procedural Lp(a) has been reported to be associated with contrast-induced acute kidney injury after emergency PCI [23]. Whether these processes extend to the renal microvasculature has not been demonstrated, and we therefore invoke them only as a putative explanation. Within that framework, iodinated contrast imposes an osmotic and viscous load on a renal medulla that already operates close to the hypoxia threshold, and a pre-existing

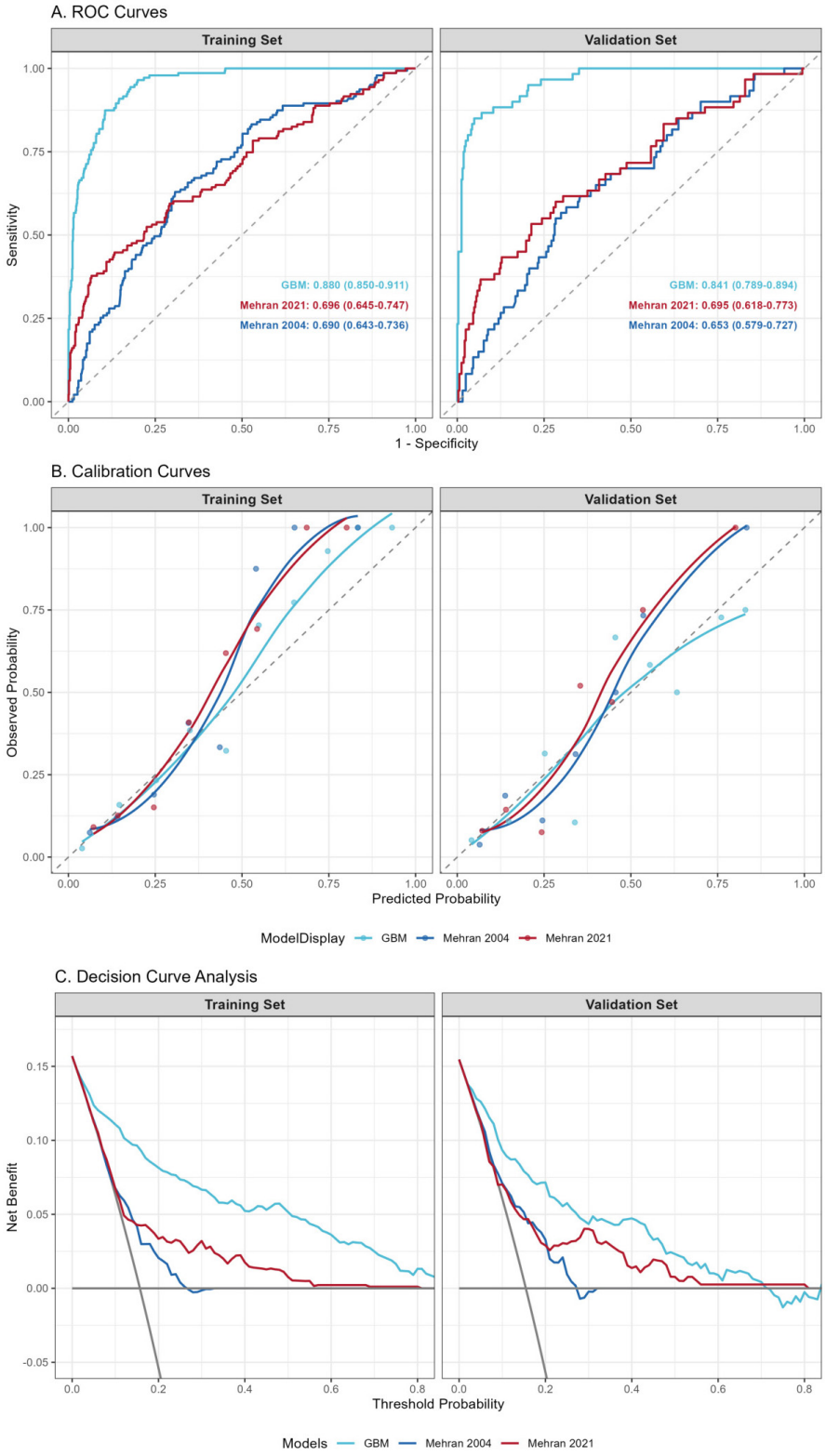


Fig. 8. Head-to-head performance comparison between the proposed GBM model, the Mehran 2004 score, and the Mehran 2021 score. Each panel shows the training set (left) and the temporal internal validation set (right). (A) Receiver operating characteristic curves; the area under the curve and its 95% confidence interval are annotated for each model. (B) Calibration curves relating predicted probability (x-axis) to observed probability (y-axis); symbols indicate observed event rates, solid lines are loess-smoothed estimates, and the dashed diagonal indicates perfect calibration. (C) Decision curve analysis; net benefit (y-axis) is plotted against the threshold probability (x-axis), the horizontal line indicates treat-none, and the descending grey line indicates treat-all. Abbreviations: AUC, area under the curve; DCA, decision curve analysis; GBM, gradient boosting machine; ROC, receiver operating characteristic.

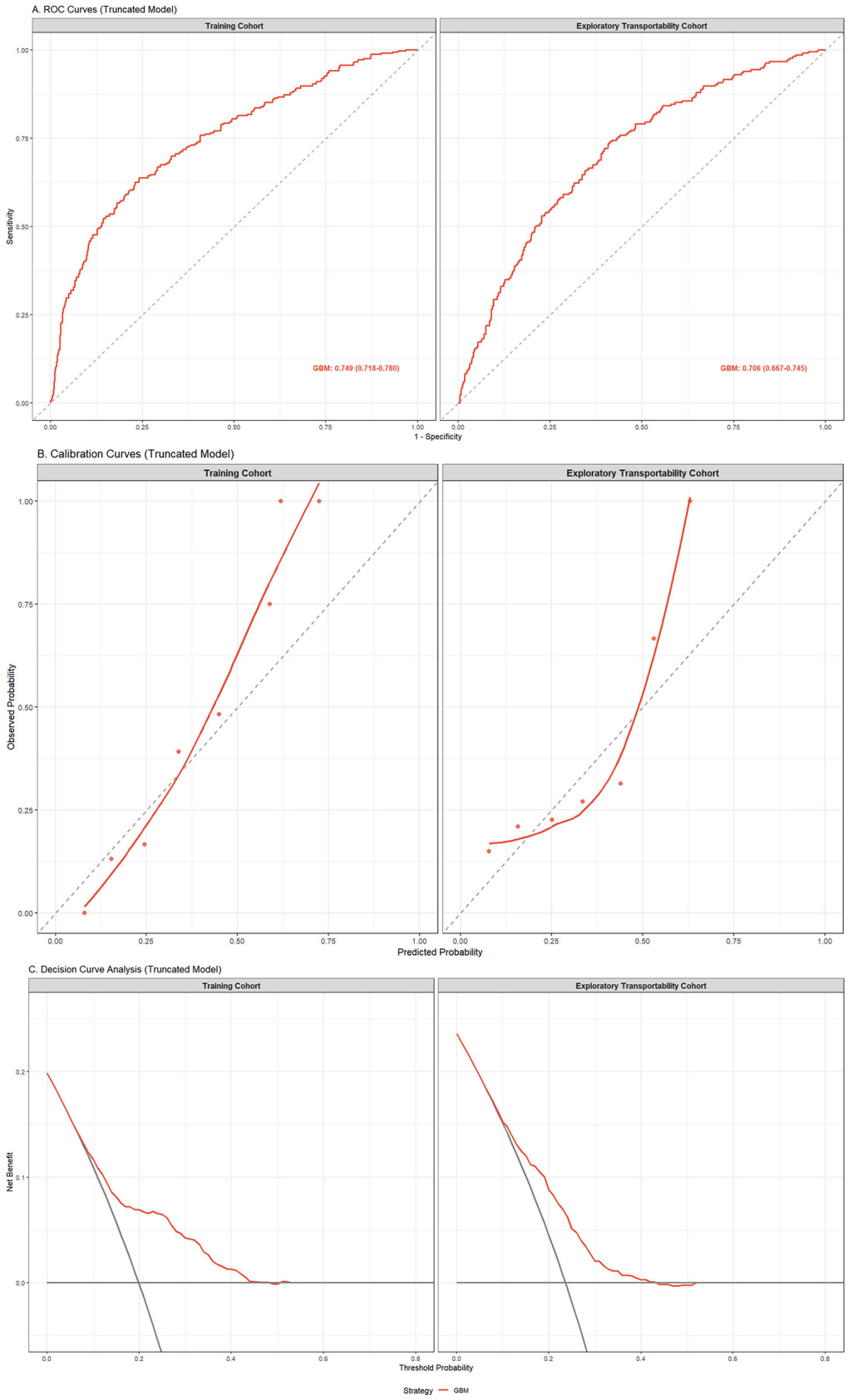


Fig. 9. Exploratory transportability analysis of the truncated GBM model in the MIMIC-IV cohort. (A) ROC curve of the 3-variable model (Age, pre-procedural eGFR, and Fasting Glucose). (B) Calibration plot. (C) Decision curve analysis (DCA). Abbreviations: DCA, decision curve analysis; eGFR, estimated glomerular filtration rate; GBM, gradient boosting machine; MIMIC-IV, Medical Information Mart for Intensive Care IV; ROC, receiver operating characteristic.

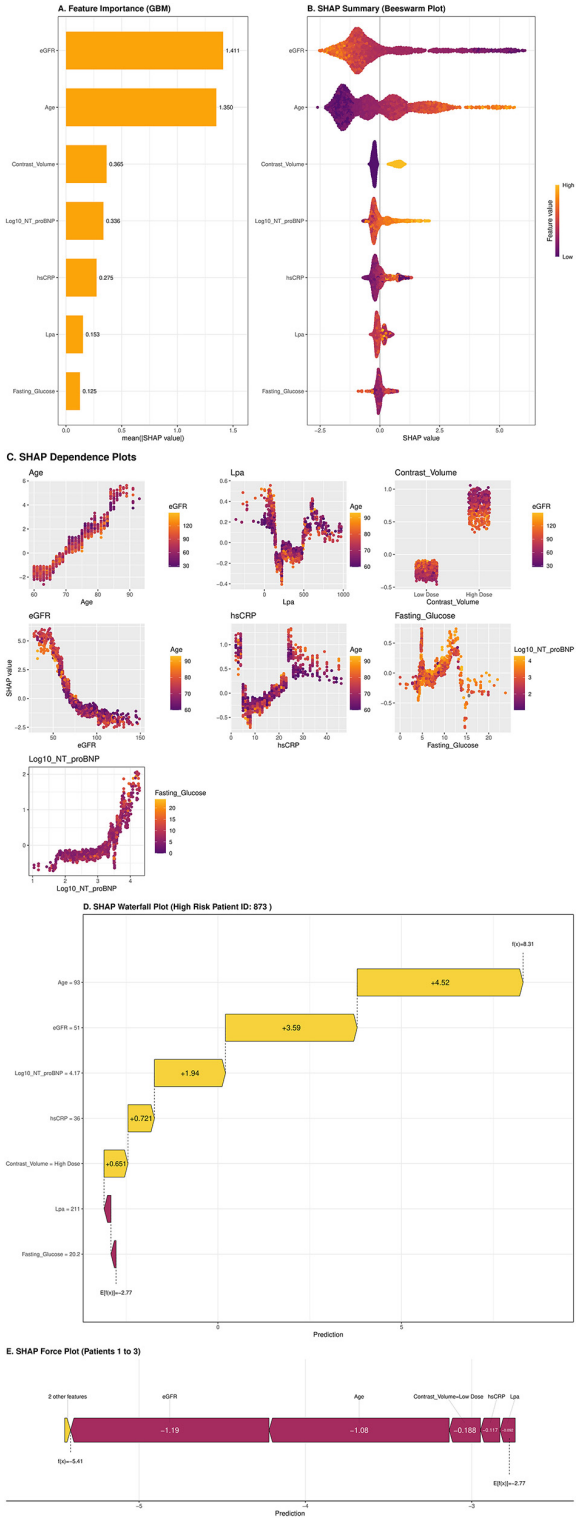


Fig. 10. SHAP-based interpretability visualizations for the optimized GBM model. (A) SHAP bar plot displaying the global importance ranking of the seven core predictors. (B) SHAP summary (beeswarm) plot depicting the distribution of SHAP values across all samples (dark purple indicates low values; yellow indicates high feature values). (C) SHAP dependence plots presenting the marginal, non-linear effects of key variables. (D,E) Individual SHAP explanations for representative high-risk (D) and low-risk (E) patients, where yellow bars indicate features increasing and pink bars features decreasing the predicted risk of CA-AKI, respectively. Abbreviations: CA-AKI, contrast-associated acute kidney injury; eGFR, estimated glomerular filtration rate; GBM, gradient boosting machine; hs-CRP, high-sensitivity C-reactive protein; Lp(a), lipoprotein(a); NT-proBNP, N-terminal pro-B-type natriuretic peptide; SHAP, SHapley Additive exPlanations.

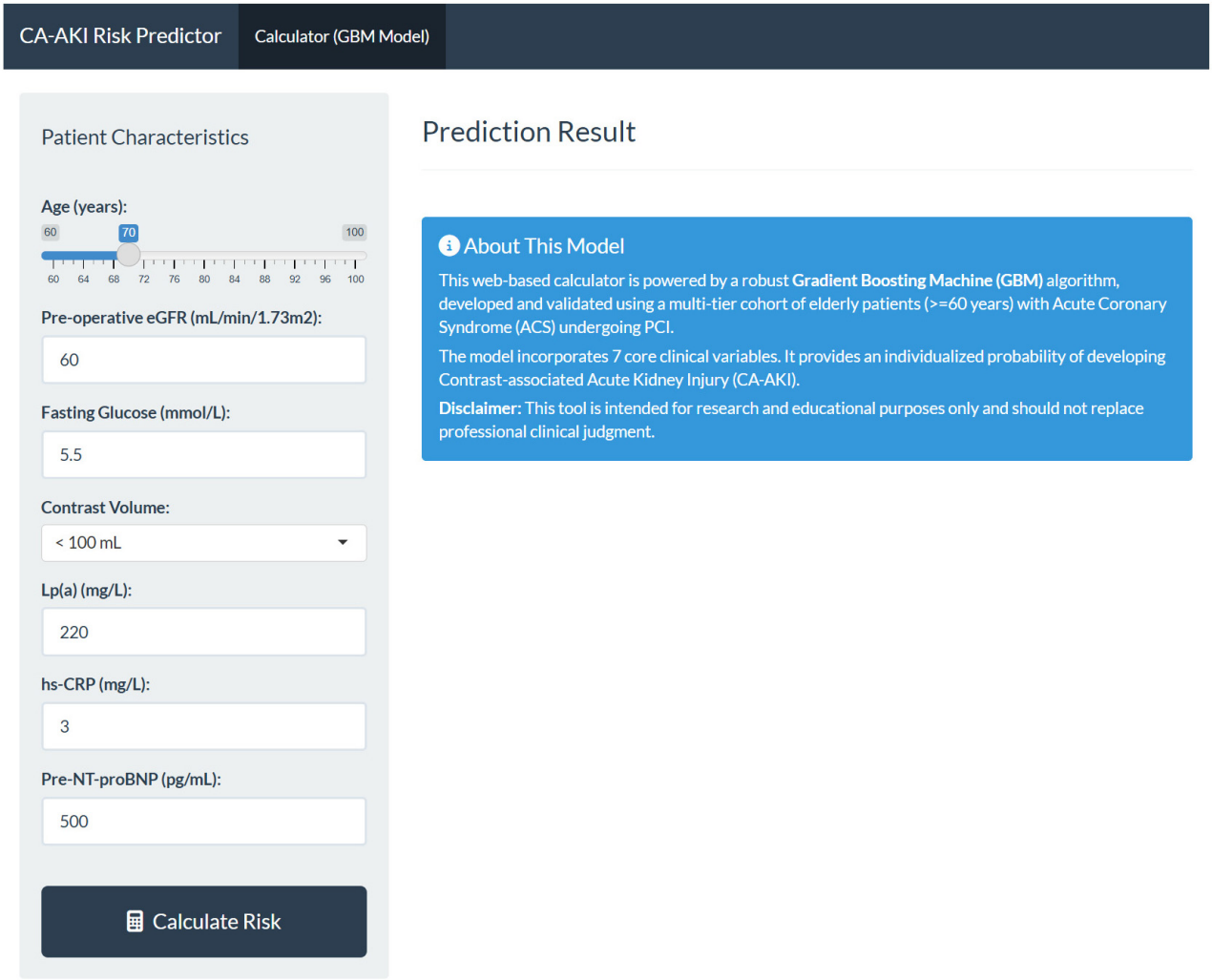


Fig. 11. Interactive web-based calculator for predicting CA-AKI in older ACS patients undergoing PCI. Abbreviations: ACS, acute coronary syndrome; CA-AKI, contrast-associated acute kidney injury; eGFR, estimated glomerular filtration rate; hs-CRP, high-sensitivity C-reactive protein; Lp(a), lipoprotein(a); NT-proBNP, N-terminal pro-B-type natriuretic peptide; PCI, percutaneous coronary intervention.

impairment of vasomotor regulation would be expected to limit compensatory vasodilation of the afferent arterioles, aggravating medullary ischaemia and downstream tubular injury [24]. Together with the haemodynamic stress captured by NT-proBNP, such a 'multiple-hit' sequence could account for the non-linear, threshold-like risk escalations detected by the GBM; this remains a pathophysiological hypothesis rather than a mechanism established by our data.

A central question in clinical translation of ML models is whether they generalize across populations. Formal transportability analysis under TRIPOD+AI guidelines requires identical feature sets [25], which is not possible when the external database lacks certain biomarkers. We addressed this through an exploratory analysis in the MIMIC-IV critical care database. The MIMIC-IV cohort differs from the primary cohort in disease severity and treatment pathways, making it a demanding test. Because Lp(a) and hs-CRP are frequently unrecorded in ICU registries, we evaluated a reduced 3-variable model using age, eGFR, and fasting glucose [26]. Even under these constraints, the simplified model retained discriminative ability [27]. This finding is clinically relevant: it indicates that the core predictors in the algorithm are stable. The systemic immune-inflammation index, which has been reported to predict CA-AKI in patients undergoing coronary angiography, was among the candidate parameters but was not retained by the feature-selection protocol [28]. The full 7-variable model is preferred when all biomarkers are available, but the reduced model can serve as a baseline assessment in settings where comprehensive panels are not accessible [29].

The clinical value of a prediction model depends on whether clinicians can use it at the point of care [30]. Translating the GBM into a free web-based calculator makes it possible to enter seven routinely available parameters and obtain a patient-specific CA-AKI probability [31]. For high-risk patients, physicians can adjust the peri-procedural

plan by intensifying hydration, limiting contrast volume, or optimizing hemodynamic support before renal injury progresses [32]. Real-world deployment ultimately hinges on laboratory turnaround times. In contemporary chest pain centers, hs-CRP and NT-proBNP serve as standard triage metrics; point-of-care testing (POCT) delivers quantitative results for these markers within 15 minutes, easily accommodating the tight schedules of emergent primary PCI. Lp(a) quantification, however, presents logistical hurdles. Slower standard assay processing and inconsistent reimbursement policies often rule out real-time risk stratification during a hyper-acute STEMI. Given these constraints, our model offers the most immediate utility for emergency patients who already have a historical Lp(a) baseline documented in their electronic medical records. For patients without prior data, the framework remains highly practical in sub-acute (e.g., NSTEMI) and elective PCI settings. These clinical pathways inherently afford a 12- to 24-hour pre-procedural window, providing clinicians with ample time to complete lipid profiling and initiate targeted prophylactic hydration.

7. Limitations

Several limitations should be noted. First, the retrospective design leaves room for unmeasured confounders, though temporal internal validation partially addresses this. Second, the study was conducted at a single center, which limits the generalizability of findings to institutions with different patient demographics or clinical pathways. Third, while 323 CA-AKI events were sufficient for model training, the overall sample size remains moderate. Overfitting is a concern; we observed it in the random forest model and chose GBM in part for its more balanced fit. Fourth, patients with incomplete core documentation (e.g., missing baseline or post-procedural creatinine) were excluded. This introduces selection bias: it may omit critically unstable patients, cardiogenic shock cases, or emergency transfers who did not receive full laboratory profiling or died before post-PCI creatinine measurement. Fifth, defining CA-AKI by serum creatinine fluctuation may cause outcome misclassification, since creatinine can be affected by transient hemodynamic instability or atheroembolism independent of contrast exposure. Sixth, unmeasured confounders from concurrent interventions, including intra-procedural hydration volume, vasoactive medications, and hemodynamic support, were not captured in the dataset and could have influenced CA-AKI development. Seventh, the decision threshold was derived statistically (Youden's index). In practice, threshold selection may require adjustment based on clinical context, risk tolerance, and institutional resources. Eighth, the model uses single-timepoint baseline data rather than longitudinal biomarker trajectories; this design was chosen to enable early bedside risk stratification before renal injury occurs. Ninth, reliance on Lp(a) limits immediate application in hyper-acute primary PCI without prior lipid records, and in settings where specialized assays are unavailable. Finally, the full 7-variable model could not be validated in MIMIC-IV because Lp(a) and hs-CRP are not routinely recorded in ICU registries. While the 3-variable validation confirmed the algorithm's baseline stability, the complete model requires prospective validation. The framework may therefore be more representative of ACS patients following a standardized peri-procedural diagnostic workflow.

8. Conclusion

This study presents a temporally validated GBM framework for predicting CA-AKI in older ACS patients, with supporting evidence of generalizability from an exploratory MIMIC-IV analysis. Seven core variables (age, eGFR, contrast volume, NT-proBNP, hs-CRP, Lp(a), and fasting glucose) were selected through a consensus feature-screening protocol. SHAP analysis clarified predictor contributions, and the model was deployed as a peri-procedural web calculator for bedside risk stratification and preventive decision-making.

Availability of Data and Materials

The individual-level clinical dataset and the analysis code are not publicly available. To comply with the relevant regulations, the author, XSZ, was certified by the Collaborative Institutional Training Initiative (CITI) and was authorized to access the MIMIC-IV database (Certificate Number: 75691658). The MIMIC-IV database used for the exploratory analysis is publicly accessible via the PhysioNet repository under its data use agreement. The complete modelling pipeline, including feature selection, hyperparameters, threshold rule and metric definitions, is specified in the Methods and **Supplementary Table 2**, and the trained model is deployed as a freely accessible interactive calculator.

Author Contributions

Conceptualization, XSZ, YX and WL; methodology, XSZ and XZ.; software, XSZ and JD; validation, JJ, SL and YX; formal analysis, XSZ and XZ; investigation, XZ and JJ; data curation, XZ, JJ and JD; writing, original draft preparation, XSZ and XZ; writing, review and editing, JJ, JD, SL, YX and WL; visualization, XSZ and JD; supervision, YX and WL; project administration, WL. All authors contributed to editorial changes in the manuscript. All authors read and approved the final manuscript. All authors have participated sufficiently in the work and agreed to be accountable for all aspects of the work.

Ethics Approval and Consent to Participate

This study was conducted under the approval of the Ethics Committee of the Affiliated Hospital of Xuzhou Medical University (XYFY-2025-KL348-01) and complied

with the Declaration of Helsinki. Given the retrospective nature of the analysis using historical medical records, the institutional review board waived the need for written informed consent. All participant data were processed anonymously to safeguard confidentiality, adhering to both national regulations and university guidelines.

Acknowledgment

Not applicable.

Funding

This research received no external funding.

Conflicts of Interest

The authors declare no conflicts of interest.

Declaration of AI and AI-Assisted Technologies in the Writing Process

During the preparation of this work, the authors used Gemini in order to improve the English language, grammar, and readability of the manuscript. After using this tool/service, the authors thoroughly reviewed and manually edited the content as needed and took full responsibility for the final content of the publication.

Supplementary Material

Supplementary material associated with this article can be found, in the online version, at https://doi.org/10.31083/RCM52089.

References

[1] Zhang L, Cao X, Yang Y, Fu S, Jia Y, Hu W, et al. Risk prediction models for contrast-induced acute kidney injury in patients with acute coronary syndromes: a systematic review and meta-analysis. Frontiers in Medicine. 2025; 12: 1629369. https://doi.org/10.3389/fmed.2025.1629369

[2] Wang Z, Wang Q, Gong X. Unveiling the Mysteries of Contrast-Induced Acute Kidney Injury: New Horizons in Pathogenesis and Prevention. Toxics. 2024; 12: 620. https://doi.org/10.3390/toxics12080620

[3] Mehran R, Aymong ED, Nikolsky E, Lasic Z, Iakovou I, Fahy M, et al. A simple risk score for prediction of contrast-induced nephropathy after percutaneous coronary intervention: development and initial validation. Journal of the American College of Cardiology. 2004; 44: 1393–1399. https://doi.org/10.1016/j.jacc.2004.06.068

[4] Arnold N, Blaum C, Goßling A, Brunner FJ, Bay B, Ferrario MM, et al. C-reactive protein modifies lipoprotein(a)-related risk for coronary heart disease: the BiomarCaRE project. European Heart Journal. 2024; 45: 1043–1054. https://doi.org/10.1093/eurheartj/ehad867

[5] Jin J, Ding J, Zhang X, Wang L, Zhang X, Li W, et al. Development and Testing a New Online Dynamic Nomogram for Contrast-Induced Acute Kidney Injury in Elderly Patients with ST-Segment Elevation Myocardial Infarction. Clinical Interventions in Aging. 2025; 20: 1085–1098. https://doi.org/10.2147/CIA.S534736

[6] Huang C, Li SX, Mahajan S, Testani JM, Wilson FP, Mena CI, et al. Development and Validation of a Model for Predicting the Risk of Acute Kidney Injury Associated With Contrast Volume Levels During Percutaneous Coronary Intervention. JAMA Network Open. 2019; 2: e1916021. https://doi.org/10.1001/jamanetworkopen.2019.16021

[7] Choi H, Choi B, Han S, Lee M, Shin GT, Kim H, et al. Applicable Machine Learning Model for Predicting Contrast-induced Nephropathy Based on Pre-catheterization Variables. Internal Medicine. 2024; 63: 773–780. https://doi.org/10.2169/internalmedicine.1459-22

[8] KDIGO Group. KDIGO clinical practice guideline for acute kidney injury. Kidney International. Supplement. 2012; 2: 1–138. https://doi.org/10.1038/kisup.2012.1

[9] Chen YF, Xu SQ, Xu YC, Li WJ, Chen KM, Cai J, et al. Inflammatory anemia may be an indicator for predicting disease activity and structural damage in Chinese patients with rheumatoid arthritis. Clinical Rheumatology. 2020; 39: 1737–1745. https://doi.org/10.1007/s10067-019-04873-y

[10] Mehran R, Owen R, Chiarito M, Baber U, Sartori S, Cao D, et al. A contemporary simple risk score for prediction of contrast-associated acute kidney injury after percutaneous coronary intervention: derivation and validation from an observational registry. Lancet. 2021; 398: 1974–1983. https://doi.org/10.1016/S0140-6736(21)02326-6

[11] Mehran R, Dangas GD, Weisbord SD. Contrast-Associated Acute Kidney Injury. The New England Journal of Medicine. 2019; 380: 2146–2155. https://doi.org/10.1056/NEJMra1805256

[12] Behnoush AH, Shariatnia MM, Khalaji A, Asadi M, Yaghoobi A, Rezaee M, et al. Predictive modeling for acute kidney injury after percutaneous coronary intervention in patients with acute coronary syndrome: a machine learning approach. European Journal of Medical Research. 2024; 29: 76. https://doi.org/10.1186/s40001-024-01675-0

[13] Sun L, Zhu W, Chen X, Jiang J, Ji Y, Liu N, et al. Machine Learning to Predict Contrast-Induced Acute Kidney Injury in Patients With Acute Myocardial Infarction. Frontiers in Medicine. 2020; 7: 592007. https://doi.org/10.3389/fmed.2020.592007

[14] Johnson AEW, Bulgarelli L, Shen L, Gayles A, Shammout A, Horng S, et al. MIMIC-IV, a freely accessible electronic health record dataset. Scientific Data. 2023; 10: 1. https://doi.org/10.1038/s41597-022-01899-x

[15] Lundberg SM, Erion G, Chen H, DeGrave A, Prutkin JM, Nair B, et al. From Local Explanations to Global Understanding with Explainable AI for Trees. Nature Machine Intelligence. 2020; 2: 56–67. https://doi.org/10.1038/s42256-019-0138-9

[16] Kursa MB, Rudnicki WR. Feature selection with the Boruta package. Journal of Statistical Software. 2010; 36: 1–13. https://doi.org/10.18637/jss.v036.i11

[17] Tibshirani R. Regression shrinkage and selection via the lasso. Journal of the Royal Statistical Society Series B: Statistical Methodology. 1996; 58: 267–288. https://doi.org/10.1111/j.2517-6161.1996.tb02080.x

[18] Friedman JH. Greedy function approximation: a gradient boosting machine. Annals of Statistics. 2001; 29: 1189–1232. https://doi.org/10.1214/aos/1013203451

[19] Zhou F, Lu Y, Xu Y, Li J, Zhang S, Lin Y, et al. Correlation between neutrophil-to-lymphocyte ratio and contrast-induced acute kidney injury and the establishment of machine-learning-based predictive models. Renal Failure. 2023; 45: 2258983. https://doi.org/10.1080/0886022X.2023.2258983

[20] Lundberg SM, Lee SI. A unified approach to interpreting model predictions. Advances in Neural Information Processing Systems. 2017; 30: 4765–4774.

[21] Boffa MB, Koschinsky ML. Oxidized phospholipids as a unifying theory for lipoprotein(a) and cardiovascular disease. Na-

ture Reviews. Cardiology. 2019; 16: 305–318. https://doi.org/10.1038/s41569-018-0153-2

[22] Wu HD, Berglund L, Dimayuga C, Jones J, Sciacca RR, Di Tullio MR, et al. High lipoprotein(a) levels and small apolipoprotein(a) sizes are associated with endothelial dysfunction in a multiethnic cohort. Journal of the American College of Cardiology. 2004; 43: 1828–1833. https://doi.org/10.1016/j.jacc.2003.08.066

[23] Tao J, Dai W, Ye C, Yao Q, Zhou M, Li Y. Preprocedural Lp(a) level and ApoB/ApoA-I ratio and the risk for contrast-induced acute kidney injury in patients undergoing emergency PCI. Lipids in Health and Disease. 2021; 20: 130. https://doi.org/10.1186/s12944-021-01535-4

[24] Persson PB, Hansell P, Liss P. Pathophysiology of contrast medium-induced nephropathy. Kidney international. 2005; 68: 14–22. https://doi.org/10.1111/j.1523-1755.2005.00377.x

[25] Collins GS, Moons KGM, Dhiman P, Riley RD, Beam AL, Van Calster B, et al. TRIPOD+AI statement: updated guidance for reporting clinical prediction models that use regression or machine learning methods. BMJ (Clinical Research Ed.). 2024; 385: e078378. https://doi.org/10.1136/bmj-2023-078378

[26] Lin S, Lu W, Wang T, Wang Y, Leng X, Chi L, et al. Predictive model of acute kidney injury in critically ill patients with acute pancreatitis: a machine learning approach using the MIMIC-IV database. Renal Failure. 2024; 46: 2303395. https://doi.org/10.1080/0886022X.2024.2303395

[27] Li J, Sun Y, Ren J, Wu Y, He Z. Machine Learning for In-hospital Mortality Prediction in Critically Ill Patients With Acute Heart Failure: A Retrospective Analysis Based on the MIMIC-IV Database. Journal of Cardiothoracic and Vascular Anesthesia. 2025; 39: 666–674. https://doi.org/10.1053/j.jvca.2024.12.016

[28] Jiang H, Li D, Xu T, Chen Z, Shan Y, Zhao L, et al. Systemic Immune-Inflammation Index Predicts Contrast-Induced Acute Kidney Injury in Patients Undergoing Coronary Angiography: A Cross-Sectional Study. Frontiers in Medicine. 2022; 9: 841601. https://doi.org/10.3389/fmed.2022.841601

[29] Li Y, Ma K, Shen G, Zheng D, Xuan Y, Li W. Impact of small and dense low-density lipoprotein (sd-LDL)on contrast-induced acute kidney injury in patients with acute ST-segment elevation myocardial infarction undergoing primary percutaneous coronary intervention. International Urology and Nephrology. 2021; 53: 2611–2617. https://doi.org/10.1007/s11255-021-02821-x

[30] Acosta JN, Falcone GJ, Rajpurkar P, Topol EJ. Multimodal biomedical AI. Nature Medicine. 2022; 28: 1773–1784. https://doi.org/10.1038/s41591-022-01981-2

[31] Kelly CJ, Karthikesalingam A, Suleyman M, Corrado G, King D. Key challenges for delivering clinical impact with artificial intelligence. BMC Medicine. 2019; 17: 195. https://doi.org/10.1186/s12916-019-1426-2

[32] Davenport MS, Perazella MA, Yee J, Dillman JR, Fine D, McDonald RJ, et al. Use of Intravenous Iodinated Contrast Media in Patients with Kidney Disease: Consensus Statements from the American College of Radiology and the National Kidney Foundation. Radiology. 2020; 294: 660–668. https://doi.org/10.1148/radiol.2019192094